IEEE Access
Multidisciplinary | Rapid Review | Open Access Journal

Received September 11, 2020, accepted September 28, 2020, date of publication October 2, 2020, date of current version October 14, 2020.

Digital Object Identifier 10.1109/ACCESS.2020.3028510

A Generalized Methodology to Generate, Amplify and Compensate Multi-Frequency Power for a Single-Inverter-Based MF-MR-S-WPT System

CHEN QI, (Member, IEEE), HAN MIAO, ZHENGYING LANG, AND XIYOU CHEN
School of Electrical Engineering, Dalian University of Technology, Dalian 116024, China

Corresponding author: Chen Qi (qichen@dlut.edu.cn)

This work was supported in part by the National Natural Science Foundation of China under Grant 51907015, and in part by the Fundamental Research Funds for the Central Universities under Grant DUT19JC07.

ABSTRACT To meet the unique challenges on how to generate, amplify and compensate the multi-frequency (MF) power in MF multi-receiver simultaneous wireless power transfer (MF-MR-S-WPT) systems, this article proposes an innovative and generalized methodology. In proposed methodology, a MF modulation method based on cosine switching frequency modulation (CSFM) technique and a general multi-resonant transmitting tank design method based on circuit synthesis theory are introduced. With the proposed MF modulation method, a standard full-bridge inverter can be used to generate MF power, leading to a simple configuration of transmitting source. Moreover, a modulation degree of freedom can be provided to change the power transfer ratio, achieving power redistribution among receivers though software implementation. With the proposed design method of multi-resonant transmitting tank, the use of complicated multiple harmonic analysis can be avoided and the arbitrary multiple power components at selected resonant frequencies can be effectively amplified and completely compensated. Finally, the effectiveness of proposed methodology is verified theoretically and experimentally.

INDEX TERMS Composite compensation, multiple frequency, switching frequency modulation, wireless power transfer.

I. INTRODUCTION

An unique feature of magnetically-coupled wireless power transfer (WPT) system is the capability of using a single transmitter to simultaneously charge multiple receivers, such as electric vehicles [1] and portable devices [2], [3]. According to whether the resonant frequencies of receivers are designed to be identical or different, the multiple-receiver simultaneous WPT (MR-S-WPT) systems can be classified into two categories: single-frequency MR-S-WPT (SF-MR-S-WPT) system [4]–[10] and multi-frequency MR-S-WPT (MF-MR-S-WPT) system [11]–[19]. In SF-MR-S-WPT system, the receivers have same resonant frequency as that of the transmitter and consequently the power transferred to different receivers is must though a common power channel. It means that the influence of cross couplings among receivers is difficult to be reduced and the power redistribution among receivers cannot be achieved by just using the transmitter [9], [10]. On the other hand, more attentions have been paid to the MF-MR-S-WPT system. In this system, the receivers are designed with different resonant frequencies. In the meantime, the transmitter provides the power of different frequencies. By tuning the resonant frequencies of receivers to one of the frequencies emitted from transmitter, the separate power channels can be established in MF-MR-S-WPT system, which would be very helpful to reduce the cross coupling influence and achieve power redistribution by just using the transmitter. However, MF-MR-S-WPT system presents unique challenges, especially on how to generate, amplify and compensate the multi-frequency (MF) power.

For generating MF power in MF-MR-S-WPT system, various inverter-based methods have been proposed. According to the number of inverters being used, these methods can be classified into two types: multi-inverter-based method [11]–[13] and single-inverter-based method [14]–[19]. In multi-inverter-based method, the multiple inverters are

The associate editor coordinating the review of this manuscript and approving it for publication was S. Ali Arefifar.

operating at different switching frequencies and can be connected to individual transformers [11], [12] or multiple transmitting coils [13] to combine MF power from transmitter to receivers. Based on this method, the power of different receivers can be controlled independently by changing the duty cycles of corresponding inverters [12]. However, the use of multiple inverters may increase system complexity and generate unexpected power losses. Instead, a single inverter can be used to generate MF power and even achieve power redistribution among receivers, leading to a relatively simple system configuration. One way of generating MF power with a single inverter is to use a modified configuration of full-bridge inverter [14], [15]. In [14] and [15], one more diode is connected in series to each inverter leg to synthesize a half-cycle sinusoidal current by applying the superposition methodology of fundamental and odd-harmonic components. In comparison with a standard full-bridge inverter, the additional diodes will increase the system loss and complexity. In addition to the modified configuration, the MF modulation methods have been presented to generate MF power for a standard full-bridge inverter [16]–[19]. The simplest MF modulation method of standard full-bridge inverter is to generate a square-waveform output voltage and the fundamental and harmonic components of this voltage can be used to simultaneously charge multiple receivers of different resonant frequencies [16], [17]. However, its disadvantages is the unchangeable component amplitude, which fails in adjusting power transfer ratio to receivers. Another MF modulation method of a standard full-bridge inverter is based on the selective harmonic elimination (SHE) technique, namely multi-frequency programmed pulse-width modulation (MFPWM) [18], [19]. In this method, the modulated full-bridge inverter can generate a dual-frequency output of 100kHz and 6.78MHz or frequencies within ranges of 87-300kHz. However, a large computational burden arises in this modulation method and therefore makes it difficult to be extended to the applications with more than two receivers. Likewise, this MF modulation method is also not a generalized one for a standard full-bridge inverter.

Except the challenge on how to generate MF power in MF-MR-S-WPT system, the amplification and compensation of MF power components are two important subjects to be further considered and their solutions are mainly based on the design of transmitting tank. Most of the configurations of transmitting tanks in the existing MF-MR-S-WPT systems are using a single series capacitor [4], [8], [11], [13], [20], [21]. This configuration is widely adopted in the single-transmitter single-receiver WPT system [22], [23], but it does not suitable to MF-MR-S-WPT system because only one resonant frequency can be provided at a time. As a result, only the selective receiver with same resonant frequency can get power and thus a simultaneous WPT cannot be achieved. To provide more resonant frequencies, a multi-resonant transmitting tank composed of multiple *LC* topologies is designed in [12], [16] and [17]. The multi-resonant tank is able to extract and amplify the power of different frequencies. Further, in [16] and [17], the reactive component at each resonant frequency is eliminated by adding a compensation tank between the multi-resonant tank and transmitting coil. However, in [12], [16] and [17], only the design process of multi-resonant transmitting tank for the case with two receivers is introduced in detail and their design methods are complicated because the multiple harmonic analysis is required. Hence, there is still a lack of simple and general design method of multi-resonant transmitting tank which can amplify and compensate the MF power components for applications with arbitrary multiple receivers.

This article demonstrates an innovative and generalized methodology to generate, amplify and compensate the MF power for a single-inverter-based MF-MR-S-WPT system, which could be easily extended to the applications with arbitrary multiple receivers. The proposed methodology has two parts: MF modulation method for a standard full-bridge and generalized design method for multi-resonant transmitting tank. The proposed MF modulation method is based on the cosine switching frequency modulation (CSFM) technique and can generate the MF power with adjustable component amplitudes. It means that a modulation degree of freedom is provided to change the power transfer ratio to receivers. The proposed general design method of multi-resonant transmitting tank is based on circuit synthesis theory and therefore can avoid the use of complicated multiple harmonic analysis. With designed tank, the MF power can be amplified to enhance power transfer level and the reactive components at each resonant frequency can be eliminated to increase system efficiency. Finally, the proposed methodology is evaluated theoretica- lly and experimentally though a sample with three receivers.

The rest of this article is organized as follows. The proposed MF-MR-S-WPT system is described in Section II. The CSFM-based MF modulation method for a standard full-bridge inverter is introduced in Section III. In Section IV, the circuit-synthesis-based general design method for multi-resonant transmitting tank is presented. The theoretical analysis of the modulated and designed system is given in Section V and experimental results are shown in Section VI. Finally, the conclusions of this article are given in Section VII.

II. THE PROPOSED MF-MR-S-WPT SYSTEM

Fig. 1 shows the circuit topology of the proposed MF-MR-S-WPT system. The system uses a standard full-bridge inverter to generate a mixed-frequency driving voltage v_{d}, which can provide power of different frequencies. Multiple receivers are designed at different resonant frequencies and each of them is tuned to one of the frequencies emitted by the MF transmitter. Consequently, the power of different frequencies from transmitter can be simultaneously transferred to multiple receivers though individual power channels of specific frequencies. In proposed system, the power transfer level of each channel can be enhanced by using a multi-resonant tank in the transmitting side. Meanwhile, the phase between

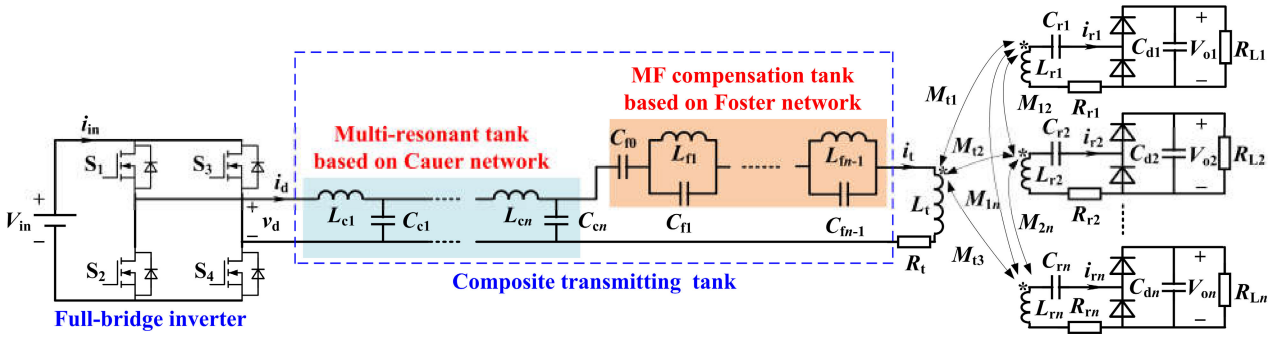

FIGURE 1. The designed MF-MR-S-WPT system using a full-bridge inverter and composite transmitting tank.

driving voltage v_d and current i_d at each resonant frequency is controlled by inserting a MF compensation tank between multi-resonant tank and transmitting coil. As shown in Fig. 1, the chosen multi-resonant tank is a combination of n LC topologies, known as Cauer network, to provide n resonant frequencies [24]. The chosen MF compensation tank is a series combination of one capacitor C_{f0} with several parallel LC topologies, known as Foster network [25]. To independently control the input phase at each resonant frequency and be guaranteed to find the positive values of Foster network parameters, the number of parallel LC topologies in Foster network should be n-1 for the system with n receivers.

In Fig.1, V_{in} and i_{in} are the input dc voltage and input current from dc source. L_{ci} and C_{ci} are the inductance and capacitance of the ith ($i = 1, \ldots, n$) LC topology in Cauer network. The inductance and capacitance of the ith LC topology in Foster network are noted as L_{fi} and C_{fi}, respectively. L_t and R_t are the self-inductance and equivalent series resistance of transmitting coil. L_{ri} and R_ri is the self-inductance and equivalent series resistance of the ith receiving coil. M_{ti} is the mutual inductance between the transmitting coil and the ith receiving coil. $M_{ij}(i = 1, \ldots, n; j = 1, \ldots, n; i \neq j)$ are the mutual inductances among receiving coils. i_t and i_{ri} are currents of transmitting coil and the ith receiving coil, respectively. C_{ri} is the series compensation capacitance of the ith receiving coil. In the ith receiver, the dc output voltage V_oi is obtained by using an uncontrollable half-bridge rectifier connecting to a filter capacitor C_{di} and feeding a passive load R_{Li}. S_i ($i = 1, 2, 3, 4$) stands for the switching signals of full-bridge inverter.

III. THE CSFM-BASED MF MODULATION METHOD

The first objective of this article is to generate the MF power by just using a single inverter. This objective can be achieved by using the MF modulation method for an inverter. As well known, the simplest single-inverter-based MF modulation method is to generate a square-waveform output voltage v_d. This MF modulation method is called the fixed switching frequency modulation (FSFM) in this article. Based on the Fourier series analysis, the v_d in FSFM can be given by

$$v_d^{FSFM}(t) = \sum_{k=1,3,5}^{\infty} F_k^{FSFM}(t) = \sum_{k=1,3,5}^{\infty} \frac{A}{k} \sin(k\omega_c t) \quad (1)$$

where $A = 4V_{in}/\pi$ and $\omega_c = 2\pi f_c$. f_c is the fixed switching frequency of inverter, which is also called the center frequency.

The frequency components of square-waveform voltage v_d, such as fundamental and third-order harmonics, can be used to simultaneously charge two receivers of different resonant frequencies [16], [17]. However, FSFM method has two drawbacks: unchangeable harmonic amplitude and large harmonic frequency difference. The former drawback may result in a nonadjustable power transfer ratio to receivers and the latter one will cause a seriously unbalanced loss distribution among receivers. To avoid these two drawbacks, a CSFM-based MF modulation method has been proposed in this article. CSFM is a kind of periodic switching frequency modulation technique and widely applied for pulse-width-modulated converters to reduce EMI [26]. This article has extended this modulation method to the MF-MR-S-WPT system.

A. BASIC SCHEME OF CSFM

In CSFM, the switching frequency of full-bridge inverter is changed in a cosine manner as

$$f(t) = f_c + K_m \cos(2\pi f_m t) \quad (2)$$

where f_m is the modulation frequency and K_m is the modulation index.

When compared with FSFM, the spectrum of driving voltage v_d in CSFM will spread into a wider frequency range with reduced harmonic amplitudes. It means each original harmonic of v_d in FSFM will be modulated by CSFM into more components of different frequencies. By using CSFM, the kth modulated harmonic of v_d is given by

$$F_k^{CSFM}(t) = \frac{A}{k} \sin[\theta_k(t)] \quad (k = 1, 3, 5, \ldots) \quad (3)$$

where θ_k is the phase angle of the kth modulated harmonic. In CFSM, θ_k is obtained by

$$\theta_k(t) = k \int_0^t 2\pi f(\tau) d\tau = k\omega_c t + km_f \sin(\omega_m t) \quad (4)$$

where $\omega_m = 2\pi f_m$. $m_f = 2\pi K_m/\omega_m$ is the modulation degree of freedom which can be used to change the component amplitudes for adjusting power transfer ratio to receivers.

Consequently, the driving voltage v_d in CSFM can be expressed by

$$v_d^{CFSM}(t) = \sum_{k=1,3,5}^{\infty} F_k^{CFSM}(t) = \sum_{k=1,3,5}^{\infty} \frac{A}{k} \sin[k\omega_c t + km_f \sin(\omega_m t)] \quad (5)$$

According to (A1) and (A2) in Appendix-A, v_d^{CFSM} showing its frequency components is derived in (6), as shown at the bottom of the next page. In (6), J_n ($n = 0, 1, \ldots$) is the nth-order Bessel function.

It can be noted in (6) that each original harmonic of v_d in FSFM is modulated by CSFM into more components with equally spaced frequencies. As clearly shown in (6), the multiple frequencies can be maintained by using the proposed CSFM-based MF modulation method. More importantly, the amplitude of each frequency component can be adjusted by changing the modulation degree of freedom m_f. It means that, based on CSFM, it is able to change power transfer ratio to receivers by just using a single inverter. Among the frequency components, those derived from the modulated fundamental F_1^{CFSM} are selected in this article because F_1^{CFSM} has a much higher amplitude than other modulated harmonics $F_k^{CFSM}(k = 3, 5, \ldots)$. Thus, the specific frequencies of individual power channels for n receivers, namely selected resonant frequencies, are chosen among the frequencies derived from F_1^{CFSM} by

$$f_i = f_c + (i-1)f_m \quad (i = 1, \ldots, n) \quad (7)$$

where f_i is the ith selected resonant frequency.

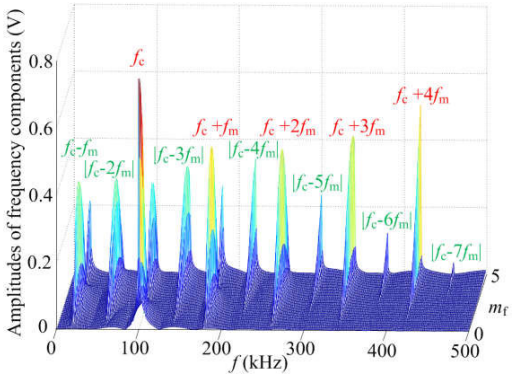

FIGURE 2. Frequency components at different values of m_f.

Fig. 2 shows the frequency components derived from F_1^{CFSM} at different values of m_f. As noted in Fig. 2, it can choose the value of m_f to change the amplitudes of frequency components whose envelopes vary in accordance with the curves of Bessel function.

B. IMPLEMENTATION OF CSFM FOR FULL-BRIDGE INVERTERS

To obtain a similar spectrum distribution as the modulated fundamental F_1^{CFSM}, the driving voltage v_d should vary

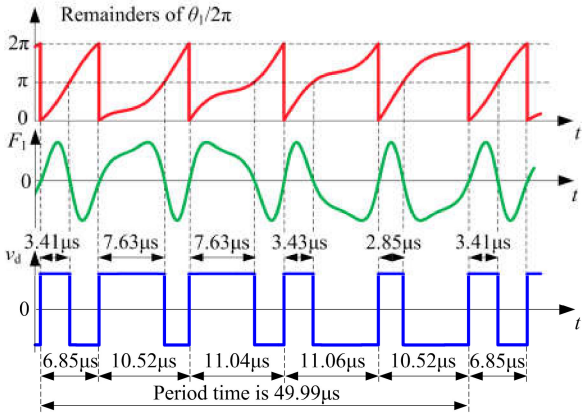

FIGURE 3. Typical waveforms in CSFM. ($m_f = 1$, $f_c = 100$kHz, $f_m = 80$kHz).

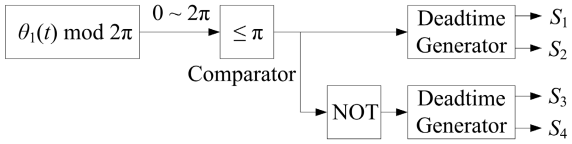

FIGURE 4. Implementation method of CSFM for full-bridge inverters.

in synchronization with F_1^{CFSM}. In other words, v_d should change at the zero-crossing instants of F_1^{CFSM}, as illustrated in Fig. 3, where m_f is set to 1.0 and f_c and f_m are set to 100kHz and 80kHz. It can be noted in Fig. 3 that the frequencies and duty cycles of pulses of v_d are different but v_d still varies in a periodic manner. The switching signals of full-bridge inverter can be generated by comparing the remainders of $\theta_1(t)/2\pi$ with π, as shown in Fig. 4.

IV. DESIGN METHODOLOGY OF COMPOSITE TRANSMITTING TANK

The second objective of proposed methodology is to amplify and compensate the MF power components. This objective can be achieved by using a composite transmitting tank, as shown in Fig. 1. The proposed composite transmitting tank is composed of multi-resonant tank and MF compensation tank. The multi-resonant tank and MF compensation tank are used to amplify and compensate the MF power components, respectively. Although the literatures [12], [16], and [17] have introduced the design method of multi-resonant tank, they require the complicated multiple harmonic analysis and does not have generality. The proposed designed method is based on circuit synthesis theory, leading to a relatively easy and more generalized task.

A. DESIGN OF MULTI-RESONANT TANK

The proposed multi-resonant tank uses the Cauer network. Fig. 5 shows the circuit model of n-order Cauer network in complex-frequency domain. The Cauer network exhibits relatively low sensitivity to nonexact values of its components, which is an important feature for WPT design.

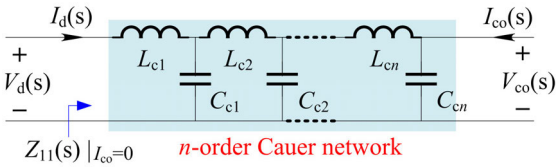

FIGURE 5. Circuit model of *n*-order Cauer network in complex-frequency domain.

The n-order Cauer network can provide n resonant frequencies and its voltage transfer function in general form can be expresses by

$$H(s) = \frac{V_{co}(s)}{V_d(s)} = H_0 \Big/ \prod_{i=1}^{n} (s^2 + \omega_i^2) \tag{8}$$

where V_d and V_{co} are the input and output voltages of Cauer network. H_0 is a constant. ω_i is the ith natural resonant angular frequency of Cauer network, at which V_{co} reach its peak value. To amplify the MF power components of selected resonant frequencies f_i, the natural resonant angular frequency ω_i of Cauer network should be chosen by

$$\omega_i = 2\pi f_i \quad (i = 1, \ldots, n) \tag{9}$$

Besides, to establish separate power channels, the resonant frequency of each receiver should be designed to one of selected resonant frequencies by tuning its series compensation capacitance C_ri as

$$C_{ri} = 1 \Big/ (4\pi^2 f_{ri} L_{ri}) \text{and } f_{ri} = f_i \tag{10}$$

where f_ri is the resonant frequency of the ith receiver.

The proposed design method of Cauer network is based on circuit synthesis of voltage transfer function $H(s)$, which can avoid the use of complicated multiple harmonic analysis. The Cauer network is a two-port LC network and its Z-parameter equation in complex-frequency domain is given by

$$\begin{bmatrix} V_d(s) \\ V_{co}(s) \end{bmatrix} = \begin{bmatrix} Z_{11}(s) & Z_{12}(s) \\ Z_{21}(s) & Z_{22}(s) \end{bmatrix} \begin{bmatrix} I_d(s) \\ I_{co}(s) \end{bmatrix} \tag{11}$$

For $I_{co} = 0$, according to (11), the voltage transfer function H(s) can be expressed by using Z parameters as

$$H(s) = \frac{V_{co}(s)}{V_d(s)} = \frac{Z_{21}(s) I_d(s)}{Z_{11}(s) I_d(s)} = \frac{Z_{21}(s)}{Z_{11}(s)} \tag{12}$$

It should be noted in (12) that the poles of $H(s)$ should be the zeros of $Z_{11}(s)$. Therefore, the circuit synthesis of $H(s)$ is to find the input impendence $Z_{11}(s)$ of Cauer network. In this article, $Z_{11}(s)$ for n-order Cauer network should be selected as

$$Z_{11}(s) = B \times \frac{\prod_{i=1}^{n} (s^2 + \omega_i^2)}{s \prod_{i=1}^{n-1} (s^2 + \omega_{pi}^2)} \tag{13}$$

where $\omega_p i (i = 1, \ldots, n-1)$ is set to $0.5(\omega_i + \omega_{i+1})$. B is the magnification coefficient. By using polynomial division, the $Z_{11}(s)$ in (13) can be transformed into

$$Z_{11}(s) = b_1 s + \cfrac{1}{b_2 s + \cfrac{1}{b_3 s + \cfrac{1}{\cdots + 1/(b_{2n} s)}}} \tag{14}$$

where $b_1 \sim b_{2\,n}$ are the constant coefficients which equal to the values of Cauer network components. In other words, L_{c1}, C_{c1}, L_{c2}, C_{c2}, $\ldots$, L_{cn}, C_{cn} in n-order Cauer network can be obtained by calculating $b_1 \sim b_{2\,n}$ as

$$L_{ci} = b_{2i-1} \quad \text{and } C_{ci} = b_{2i} \quad (i = 1, \ldots, n) \tag{15}$$

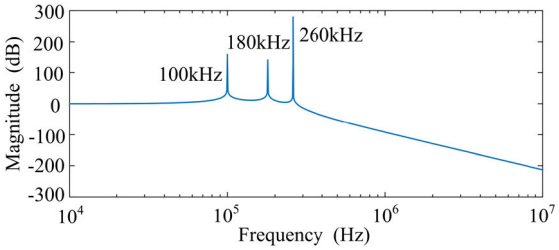

FIGURE 6. Bode figure of voltage transfer function of 3-order Cauer network.

Fig. 6 shows the bode figure of voltage transfer function $H(s)$, where a 3-order Cauer network is illustrated and its parameters are calculated in (15). Here, three resonant frequencies are chosen to $f_1 = 100$kHz, $f_2 = 180$kHz, and $f_3 = 260$kHz, respectively. The magnification coefficient B in (13) is chosen to $2/\pi/f_1$. As shown in Fig. 6, the designed Cauer network can amplify its output voltage at each selected resonant frequency and further establish separate power channels with an enhanced power transfer level.

$$\left.\begin{aligned} & v_d^{\mathrm{CSFM}}(t) = AJ_0(m_f)\sin(\omega_c t) \\ & +AJ_1(m_f)\{\sin[(\omega_c+\omega_m)t] - \sin[(\omega_c-\omega_m)t]\} \\ & +AJ_2(m_f)\{\sin[(\omega_c+2\omega_m)t] + \sin[(\omega_c-2\omega_m)t]\} \\ & +AJ_3(m_f)\{\sin[(\omega_c+3\omega_m)t] - \sin[(\omega_c-3\omega_m)t]\} \\ & +\cdots\cdots \end{aligned}\right\} F_1^{\mathrm{CSFM}}(t)$$

$$\left.\begin{aligned} & A/k \times J_0(km_f)\sin(k\omega_c t) \\ & +A/k \times J_1(km_f)\{\sin[(k\omega_c+\omega_m)t] - \sin[(k\omega_c-\omega_m)t]\} \\ & +A/k \times J_2(km_f)\{\sin[(k\omega_c+2\omega_m)t] + \sin[(k\omega_c-2\omega_m)t]\} \\ & +A/k \times J_3(km_f)\{\sin[(k\omega_c+3\omega_m)t] - \sin[(k\omega_c-3\omega_m)t]\} \\ & +\cdots\cdots \end{aligned}\right\} F_k^{\mathrm{CSFM}}(t) \tag{6}$$

B. DESIGN OF MF COMPENSATION TANK

Although the use of Cauer network as multi-resonant tank is able to amplify the MF power at selected resonant frequencies, it cannot compensate the reactive components. In this article, a MF compensation tank based on Foster network is inserted between multi-resonant tank and transmitting coil to eliminate reactive component at each selected resonant frequency and its general design method is introduced as follows.

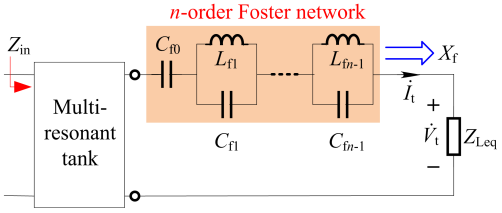

FIGURE 7. Circuit model of *n*-order Foster network.

Fig. 7 shows the circuit model of n-order Foster network, where X_{f} represents the equivalent reactance of Foster network. Z_{Leq} is the equivalent load impendence reflected from multiple receivers and can be expressed by applying Cramer's rule as

$$Z_{\mathrm{Leq}} = D/A_1 \tag{16}$$

where D and A_1 are the determinants of coefficient matrix and can be calculated in (A5) and (A6), respectively.

According to circuit theory, the input impendence Z_{in} of system can be obtained by

$$Z_{\mathrm{in}} = \frac{T_{11}(Z_{\mathrm{Leq}} + \mathrm{j}X_{\mathrm{f}}) + T_{12}}{T_{21}(Z_{\mathrm{Leq}} + \mathrm{j}X_{\mathrm{f}}) + T_{22}} \tag{17}$$

where T_{ij} ($i = 1, 2$ and $j = 1, 2$) is the T parameter of Cauer network, which can be calculated in (A7).

The expected equivalent reactance X_{f}^* of Foster network, at which the imaginary part of Z_{in} becomes zero, can be yielded by solving (18).

$$\mathrm{Im}\left[\frac{T_{11}(Z_{\mathrm{Leq}} + \mathrm{j}X_{\mathrm{f}}^*) + T_{12}}{T_{21}(Z_{\mathrm{Leq}} + \mathrm{j}X_{\mathrm{f}}^*) + T_{22}}\right] = 0 \tag{18}$$

However, it is difficult to get the analytical solutions because the order of (18) is high. Therefore, instead of the analytical solutions, the numerical solutions of (18) can be used to find X_{f}^*.

For the MF-MR-S-WPT system with n receivers, n different selected resonant frequencies $f_1, f_2, \ldots, f_n$ are required and can be chosen in (7). To independently control the input phase at each selected resonant frequency, the Forster network needs to provide n different values of X_{f}^* responding to n selected resonant frequencies. That is, $X_{\mathrm{f}}^*(\omega_1), X_{\mathrm{f}}^*(\omega_2), \ldots, X_{\mathrm{f}}^*(\omega_n)$. For n-order Foster network shown in Fig. 7, its equivalent reactance X_{f} is expressed as

$$X_{\mathrm{f}} = \frac{-1}{\omega C_{\mathrm{f0}}} + \sum_{i=1}^{n-1} \frac{\omega L_{\mathrm{f}i}}{1 - \omega^2 L_{\mathrm{f}i} C_{\mathrm{f}i}} \tag{19}$$

It can be noted that in (19) that the Foster network has the feasibility of compensating both inductive and capacitive reactive components because the equivalent reactance $\omega L_{\mathrm{fi}}/(1\text{-}\omega^2 L_{\mathrm{fi}} C_{\mathrm{fi}})$ of one parallel LC topology in Foster network can be designed to be positive or negative value. That is why the Foster network (a series combination of one capacitor with several parallel LC topologies) is chosen as the MF compensation tank in this article because it has generality for compensating reactive component of any value. As noted in (19), the adding of one parallel LC topology in Foster network has the potential to provide one more different value of X_{f}. To provide n different values of X_{f} for independent control of input phase at all selected resonant frequencies and be guaranteed to find the positive value of Foster network parameters, the number of parallel LC topologies in Foster network should be n-1 for the system with n receivers. The component parameters of Foster network can be determined in the following steps.

Step1: Determine the denominator $1\text{-}\omega^2 L_{\mathrm{fi}} C_{\mathrm{fi}}$ in (19) by choosing the product term $L_{\mathrm{fi}} C_{\mathrm{fi}}$ to be a certain value. In this article, $L_{\mathrm{fi}} C_{\mathrm{fi}}$ is chosen to p/ω_i^2. ω_i is the ith selected resonant angular frequency, given in (9). p is a constant. For example, p can be chosen as 0.95. If the calculated component parameters of Foster network are negative, p is changed to be more than 1. Here, p can be chosen as 1.05.

Step2: Substitute $L_{\mathrm{fi}} C_{\mathrm{fi}} = p/\omega_i^2$ to (19) and establish the following linear equation considering X_{f}^* at n selected resonant frequencies.

$$\begin{bmatrix} X_{\mathrm{f}}^*(\omega_1) \\ X_{\mathrm{f}}^*(\omega_2) \\ \vdots \\ X_{\mathrm{f}}^*(\omega_n) \end{bmatrix} = \boldsymbol{X} \begin{bmatrix} 1/C_{\mathrm{f0}} \\ L_{\mathrm{f1}} \\ \vdots \\ L_{\mathrm{fn}} \end{bmatrix} \tag{20}$$

where $\boldsymbol{X}$ is the $n \times n$ coefficient matrix and can be expressed by

$$\boldsymbol{X} = \begin{bmatrix} \dfrac{-1}{\omega_1} & \dfrac{\omega_1}{1-p} & \cdots & \dfrac{\omega_1}{1-p\omega_1^2/\omega_n^2} \\ \dfrac{-1}{\omega_2} & \dfrac{\omega_2}{1-p\omega_2^2/\omega_1^2} & \cdots & \dfrac{\omega_2}{1-p\omega_2^2/\omega_n^2} \\ \vdots & \vdots & \ddots & \vdots \\ \dfrac{-1}{\omega_n} & \dfrac{\omega_n}{1-p\omega_n^2/\omega_1^2} & \cdots & \dfrac{\omega_n}{1-p} \end{bmatrix} \tag{21}$$

The C_{f0} and L_{f1} to L_{fn} can be calculated by

$$\begin{bmatrix} 1/C_{\mathrm{f0}} \\ L_{\mathrm{f1}} \\ \vdots \\ L_{\mathrm{fn}} \end{bmatrix} = \boldsymbol{X}^{-1} \begin{bmatrix} X_{\mathrm{f}}^*(\omega_1) \\ X_{\mathrm{f}}^*(\omega_2) \\ \vdots \\ X_{\mathrm{f}}^*(\omega_n) \end{bmatrix} \tag{22}$$

Step 3: Calculate the rest of components C_{f1} to C_{fn} by

$$C_{\mathrm{fi}} = \frac{p}{\omega_i^2 L_{\mathrm{fi}}} \quad (i = 1, \ldots, n-1) \tag{23}$$

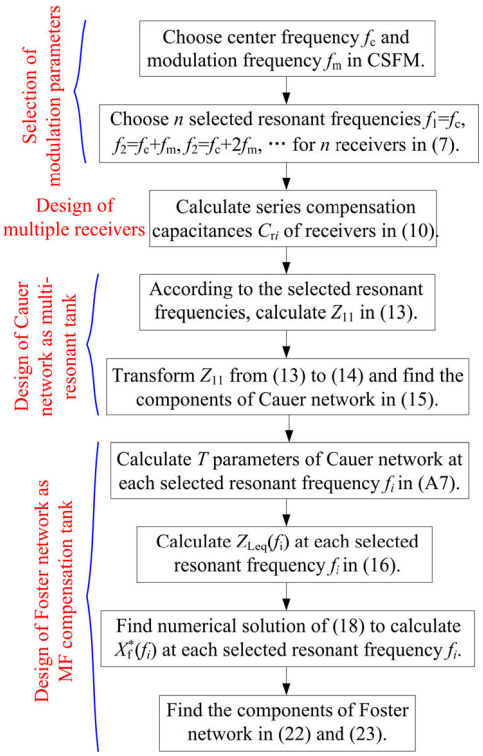

FIGURE 8. Design flow of the whole system.

C. DESIGN FLOW OF THE WHOLE SYSTEM

Fig. 8 shows the generalized design flow of the whole system. At first, the center frequency f_c and modulation frequency f_m are chosen to determine the selected resonant frequencies f_i ($i = 1, \ldots, n$) in (7), which are emitted from MF transmitter. And then, the resonant frequencies of receivers are designed to the selected resonant frequencies by tuning the series compensation capacitances C_ri in (10). Next, the power channels to couple transmitter with receivers though multi-resonant tank are established by choosing the natural resonant frequencies of Cauer network to the selected resonant frequencies. Based on the circuit synthesis of input impedance Z_{11}, the components of Cauer network can be found in (15). Lastly, according to the expected equivalent reactance of Foster network at each selected resonant frequency, the components of Foster network can be found in (22) and (23).

V. THEORETICAL ANALYSIS OF PROPOSED SYSTEM

A. INPUT IMPENDENCE

For simplifying the theoretical analysis, the proposed system with three receivers is considered as a representative example and its equivalent circuit at any single one angular frequency ω is given in Fig. 9, where the input impendence $Z_{in}^{(\omega)}$ without using the designed transmitting tank, with just using the designed multi-resonant tank, and with simultaneously using the designed multi-resonant tank and MF compensation tank are calculated, respectively.

Fig. 10 shows the calculated angles of $Z_{in}^{(\omega)}$ at different frequencies and the specifications are listed as follows: V_{in} = 30V, $f_1 = f_{r1} = 100$kHz, $f_2 = f_{r2} = 180$kHz, $f_3 = f_{r3} = 260$kHz, $B = 2/\pi/f_1$, $L_t = 75\mu$H, $R_t = 0.3\Omega$, $L_{r1} = L_{r2} = L_{r3} = 25\mu$H, $M_{t1} = M_{t2} = M_{t3} = 3\mu$H, $M_{12} = M_{13} = M_{23} = 1\mu$H, $R_{r1} = R_{r2} = R_{r3} = 0.1\Omega$, and $R_{L1} = R_{L2} = R_{L3} = 5\Omega$. Then, according to the design flow in Fig. 8, the parameters of designed transmitting tank are calculated and listed as follows: $R_{rec1} = R_{rec2} = R_{rec3} = 2.03\Omega$, $C_{r1} = 101.32$nF, $C_{r2} = 31.27$nF, $C_{r3} = 14.99$nF, $L_{c1} = 6.37\mu$H, $L_{c2} = 18.28\mu$H, $L_{c3} = 57.94\mu$H, $C_{c1} = 94.74$nF, $C_{c2} = 57.33$nF, $C_{c3} = 20.27$nF, $C_{f0} = 14.74$nF, $L_{f1} = 6.24\mu$H, $C_{f1} = 103.57$nF, $L_{f2} = 2.19\mu$H, and $C_{f2} = 211.13$nF. As noted in Fig. 10, by using the designed MF compensation tank, the angles of $Z_{in}^{(\omega)}$ at each selected resonant frequency become zero. It means that the MF reactive components through separate power channels are completely eliminated.

As shown in Fig. 10, although the MF compensation tank is designed to eliminate the reactive components at selected resonant frequencies, it fails in controlling the phase between driving voltage v_d and current i_d to zero at all frequencies, such as sideband frequencies f_c-f_m, $|f_c$-$2f_m|$, and $|f_c$-$3f_m|$, and

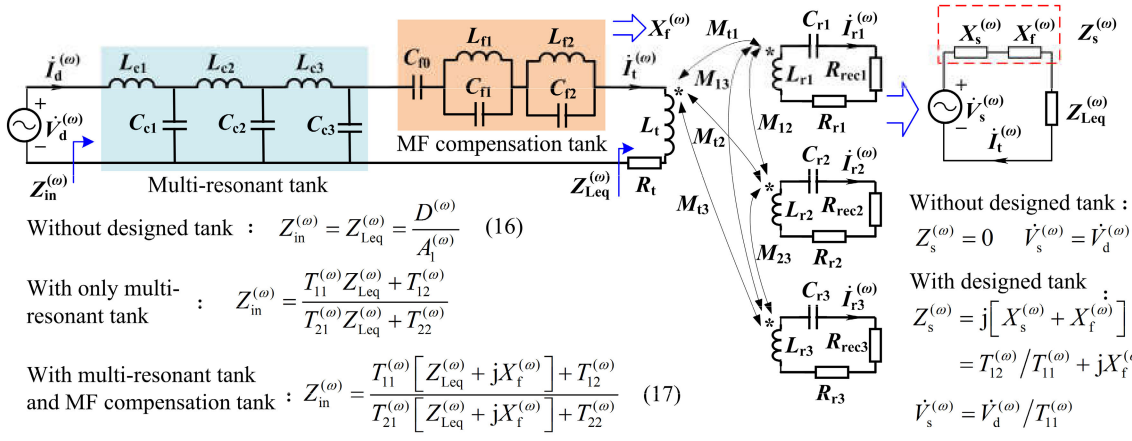

FIGURE 9. The equivalent circuit of proposed system with three receivers at any single one angular frequency ω.

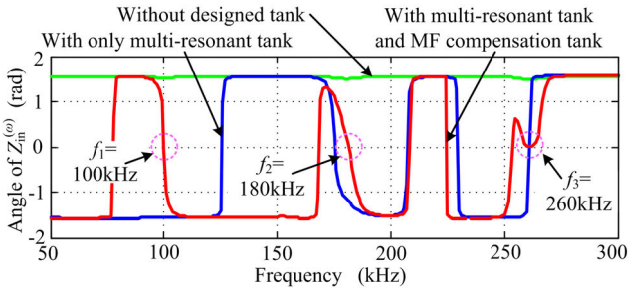

FIGURE 10. Calculated angles of $Z_{\text{in}}^{(\omega)}$ at different frequencies.

so on. As a result, the zero-current switching of inverter cannot be maintained all the time. Nevertheless, switching losses caused by non-selected frequency components are small because the majority of power transferred to receivers is through individual power channels of selected resonant frequencies. For this reason, the reactive power at non-selected frequencies is also small.

B. OUTPUT POWER

By using the Thevenin's theorem and considering the total equivalent impedance, the circuit form in Fig. 9 changes from the left-side compound circuit to the right-side simple one. As previously addressed, $X_{\text{f}}^{(\omega)}$ represents the equivalent reactance of MF compensation tank. $\dot{V}_s^{(\omega)}$ and $X_s^{(\omega)}$ represent the Thevenin equivalent voltage source and impedance, respectively, looking from the output terminals of multi-resonant tank.

By applying Cramer's rule, three receiving coil current phasors $\dot{I}_{\text{r1}}^{(\omega)}$, $\dot{I}_{\text{r2}}^{(\omega)}$, and $\dot{I}_{\text{r3}}^{(\omega)}$ are calculated by

$$\dot{I}_{\text{r1}}^{(\omega)} = -\frac{A_2^{(\omega)}}{D_{\text{s}}^{(\omega)}}\dot{V}_{\text{s}}^{(\omega)}, \quad \dot{I}_{\text{r2}}^{(\omega)} = -\frac{A_3^{(\omega)}}{D_{\text{s}}^{(\omega)}}\dot{V}_{\text{s}}^{(\omega)},$$
$$\dot{I}_{\text{r3}}^{(\omega)} = -\frac{A_4^{(\omega)}}{D_{\text{s}}^{(\omega)}}\dot{V}_{\text{s}}^{(\omega)} \tag{24}$$

where

$$D_{\text{s}}^{(\omega)} = \begin{vmatrix} Z_{\text{s}}^{(\omega)} + Z_t^{(\omega)} & \text{j}\omega M_{\text{t1}} & \text{j}\omega M_{\text{t2}} & \text{j}\omega M_{\text{t3}} \\ \text{j}\omega M_{\text{t1}} & Z_{\text{r1}}^{(\omega)} & \text{j}\omega M_{\text{t2}} & \text{j}\omega M_{\text{t3}} \\ \text{j}\omega M_{\text{t2}} & \text{j}\omega M_{12} & Z_{\text{r2}}^{(\omega)} & \text{j}\omega M_{23} \\ \text{j}\omega M_{\text{t3}} & \text{j}\omega M_{13} & \text{j}\omega M_{23} & Z_{\text{r3}}^{(\omega)} \end{vmatrix} \tag{25}$$

$$A_2^{(\omega)} = \begin{vmatrix} \text{j}\omega M_{\text{t1}} & \text{j}\omega M_{12} & \text{j}\omega M_{13} \\ \text{j}\omega M_{\text{t2}} & Z_{\text{r2}}^{(\omega)} & \text{j}\omega M_{23} \\ \text{j}\omega M_{\text{t3}} & \text{j}\omega M_{23} & Z_{\text{r3}}^{(\omega)} \end{vmatrix} \tag{26a}$$

$$A_3^{(\omega)} = \begin{vmatrix} \text{j}\omega M_{\text{t1}} & Z_{\text{r1}}^{(\omega)} & \text{j}\omega M_{13} \\ \text{j}\omega M_{\text{t2}} & \text{j}\omega M_{12} & \text{j}\omega M_{23} \\ \text{j}\omega M_{\text{t3}} & \text{j}\omega M_{13} & Z_{\text{r3}}^{(\omega)} \end{vmatrix} \tag{26b}$$

$$A_4^{(\omega)} = \begin{vmatrix} \text{j}\omega M_{\text{t1}} & Z_{\text{r1}}^{(\omega)} & \text{j}\omega M_{12} \\ \text{j}\omega M_{\text{t2}} & \text{j}\omega M_{12} & Z_{\text{r2}}^{(\omega)} \\ \text{j}\omega M_{\text{t3}} & \text{j}\omega M_{13} & \text{j}\omega M_{23} \end{vmatrix} \tag{26c}$$

With using the designed transmitting tank, the output power of the kth receiver at any single one angular frequency ω is obtained by

$$P_{\text{ok}}^{(\omega)} = \frac{R_{\text{reck}}}{2} \times \left|\dot{I}_{\text{rk}}^{(\omega)}\right|^2 = \frac{R_{\text{reck}}}{2} \times \left|\frac{A_{k+1}^{(\omega)}}{D_{\text{s}}^{(\omega)} T_{11}^{(\omega)}}\right|^2 \times \left|\dot{V}_{\text{d}}^{(\omega)}\right|^2 \tag{27}$$

According to (6), by using CSFM, the absolution value of driving voltage phasor at the ith selected resonant frequency can be given by

$$\left|\dot{V}_{\text{d}}^{(\omega_i)}\right| = \frac{4V_{\text{in}}}{\pi}|J_{i-1}(m_{\text{f}})| \quad (i = 1, \ldots, n) \tag{28}$$

Substituting (28) into (27), the output power of the kth receiver at the ith selected resonant frequency is given by

$$P_{\text{ok}}^{(\omega_i)} = \frac{8V_{\text{in}}^2[J_{i-1}(m_{\text{f}})]^2 R_{\text{reck}}}{\pi^2} \times \left|\frac{A_{k+1}^{(\omega_i)}}{D_{\text{s}}^{(\omega_i)} T_{11}^{(\omega_i)}}\right|^2 \tag{29}$$

Based on the multi-frequency multi-magnitude superposition methodology of power components at selected resonant frequencies, the total output power of the kth receiver by applying the CSFM can be given by

$$P_{\text{ok}}^{\text{Total}} = \sum_{i=1}^{n} P_{\text{ok}}^{(\omega_i)} \approx P_{\text{ok}}^{(\omega_k)} \tag{30}$$

By tuning the resonant frequencies of receivers to one of the frequencies emitted from transmitter, the separate power channels are established in MF-MR-S-WPT system. Consequently, the vast majority of power transferred to receivers is through individual power channels of selected resonant frequencies and therefore the total output power of receiver is approximated to the output power only at itself resonant frequency. So, the expression of output power of receiver in (30) can be simplified. Moreover, it can be noted in (29) that by using the proposed CSFM, the output power of receivers can be adjusted by changing the modulation degree of freedom m_{f}. Fig. 11 shows the calculated total and approximate output power of three receivers at different values of m_{f}, with and without using the designed transmitting tank. For the case without using the designed transmitting tank, the output power can be calculated similarly by using (29) and (30), but here $D_{\text{s}}^{(\omega_i)}$ in (29) should be replaced by $D^{(\omega_i)}$ which is given in (A5) and $T_{11}^{(\omega_i)}$ in (29) should be set to be one instead. As shown in Fig. 11 (a) and (b), regardless of whether it uses or does not use the designed transmitting tank, the curves of total and approximate output power of receivers have a good coincidence. Nevertheless, comparing Fig. 11 (b) with Fig. 11 (a), the power transfer level is enhanced greatly with using the designed multi-resonant tank. It means that the MF power through separate power channels is amplified.

VI. EXPERIMENTAL RESULTS

To verify the validity of proposed system and corresponding MF modulation method and general design method, a setup of the system with three receivers is built in the laboratory, as shown in Fig. 12. The proposed CSFM

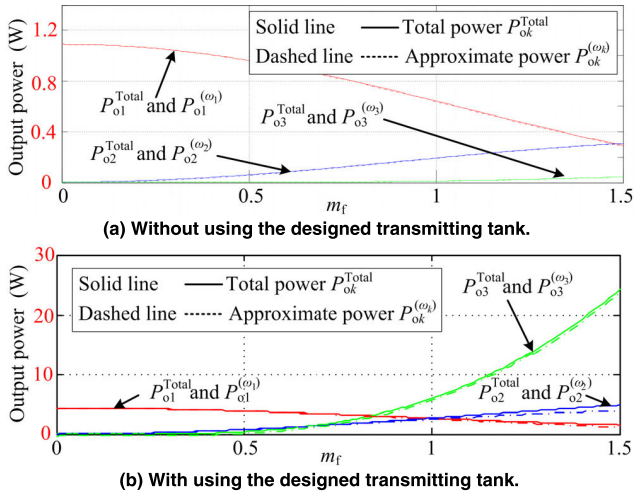

FIGURE 11. Calculated output power of receivers at different m_f.

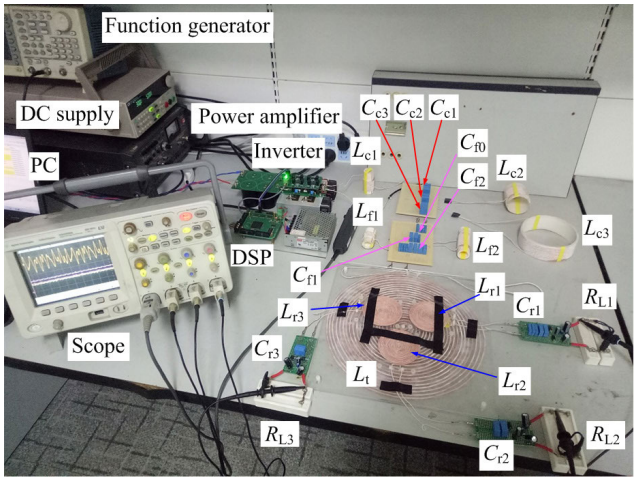

FIGURE 12. Experimental setup of proposed system with three receivers.

method for full-bridge inverters is implemented using DSP TMS320F28335. The waveforms and data are recorded by the oscilloscope (Agilent DSO 5034A). The parameters of the system are measured by using an LCR meter (HIOKI 3532-50) and listed in Table 1. The system will be tested in two steps. In the first step, to clearly demonstrate the effectiveness of power amplification and reactive compensation with using the designed transmitting tank, the system is tested at single selected resonant frequency. Here, the driving voltage is sinusoidal and can be provided through the function generator (Tektronix AFG3022) and power amplifier (NF HSA4012). Then, the system is tested at all selected resonant frequencies to verify the MF power generation and power redistribution among receivers. Instead, the transmitting composite compensation is connected to a full-bridge inverter which is modulated by using CSFM to provided a MF driving voltage with adjustable component amplitudes. The input voltage of full-bridge inverter is generated by a dc supply (IT6723H).

TABLE 1. Experimental specifications.

	Parameter	Value	Unit
DC supply	V_{in}	30	V
Inverter	Deadtime	200	ns
CSFM	f_c	100	kHz
	f_m	80	kHz
Selected resonant frequencies	f_1 / f_2 / f_3	100/180/260	kHz
Cauer network	L_{c1} / L_{c2} / L_{c3}	6.2/18.1/58.2	μH
	C_{c1} / C_{c2} / C_{c3}	95.1/57.2/20.1	nF
Foster network	C_{f0} / C_{f1} / C_{f2}	16.5/69.5/122.5	nF
	L_{f1} / L_{f2}	9.3/2.5	μH
Transmitting coil	L_t	54.4	μH
	R_t	0.12	Ω
Receiving coil	L_{r1} / L_{r2} / L_{r3}	12.2/12.7/13.1	μH
	R_{r1} / R_{r2} / R_{r3}	0.06/0.07/0.07	Ω
Coupler	M_{t1} / M_{t2} / M_{t3}	3.63/3.9/3.83	μH
	M_{12} / M_{13} / M_{23}	0.21/0.19/0.22	μH
Receivers	C_{r1} / C_{r2} / C_{r3}	207.6/61.5/28.6	nF
	C_{d1} / C_{d2} / C_{d3}	1.04/1.04/1.04	mF
Loads	R_{L1} / R_{L2} / R_{L3}	5.05/5.1/5.03	Ω

A. VERIFICATION OF MF POWER AMPLIFICATION AND COMPENSATION

Fig. 13 shows the experimental waveforms of the proposed system tested at single selected resonant frequency, where three resonant frequencies for the system with three receivers are chosen to $f_1 = 100$kHz, $f_2 = 180$kHz, and $f_3 = 260$kHz, respectively. As shown in Fig. 13 (a), (c), and (e), the phase angles between driving voltage v_d and driving current i_d at each selected resonant frequency are compensated to be very close to zero by using the designed MF compensation tank. It can be noted in Fig. 13 (b), (d) and (f) that the output voltage of the receiver at itself selected resonant frequency is much higher than other two output voltages. That means the designed multi-resonant tank can extract and amplify the MF power at selected resonant frequencies and then establish the separate power channels. As observed in Fig. 13 (e) and (f), a small driving voltage at the third resonant frequency can be used to generated a relatively large output voltage. This is because the voltage gain of the design multi-resonant tank at that frequency is much higher than others at different selected resonant frequencies, as shown in Fig. 6.

It can be noted in Fig. 13 that when the system is operating at single selected resonant frequency, only the receiver which has same resonant frequency can get power and others can hardly be charged. It means that the influence of the cross coupling among receivers is less. There are two reasons. One is the receivers in experiments are placed without overlapping and therefore the mutual inductances among receiving coils are much smaller than that between transmitting coil and receiving coils. The other reason is that by introducing the multi-frequency concept to establish separate power channels, the cross coupling influence is inherently reduced.

B. VERIFICATION OF MF POWER GENERATION

Fig. 14 shows the measured spectrum of driving voltage v_d using CSFM at three different values of m_f. When m_f is

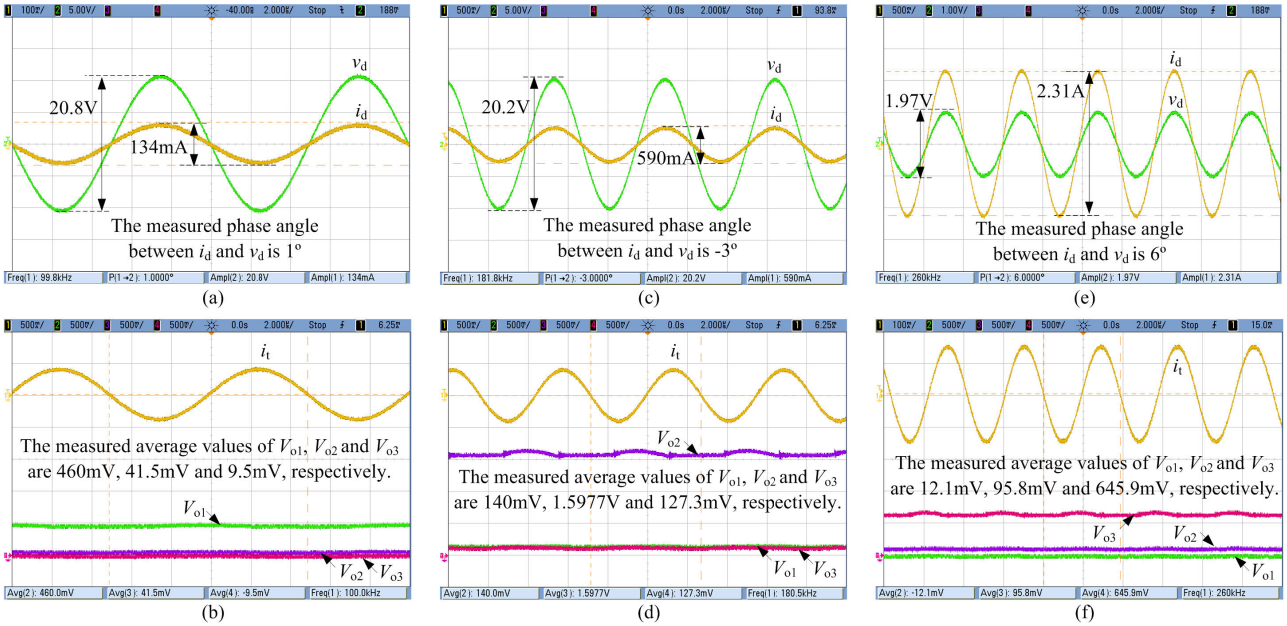

FIGURE 13. Experimental waveforms of the system tested at single selected resonant frequency ((a) and (b): 100kHz; (c) and (d): 180kHz; (e) and (f): 260kHz).

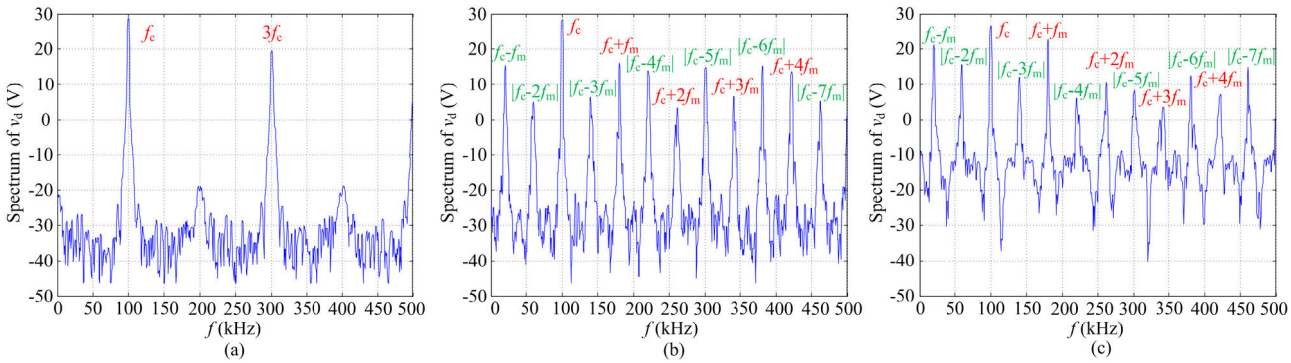

FIGURE 14. Measured spectrum of driving voltage v_d using CSFM at three different values of m_f((a): $m_f = 0$; (b): $m_f = 0.5$; (c): $m_f = 1$).

set to be zero, CSFM becomes FSFM. As analyzed in (6), the original harmonic of v_d in FSFM is modulated by CSFM into more components with equally spaced frequencies and it can choose the value of m_f to change the amplitudes of frequency components.

Fig. 15 shows the experimental waveforms of the proposed system tested by using CSFM at two different values of m_f. The pulses of driving voltage v_d in CSFM have a variable frequency and duty cycle, which excite the MF driving current i_d as well as MF transmitting current i_t. When m_f is 0.5, as shown in Fig. 14 (b), the frequency component of v_d at first selected resonant frequency $f_1 = f_c$ is much higher than those at other two selected resonant frequencies $f_2 = f_c + f_m$ and $f_3 = f_c + 2f_m$. Therefore, the output voltage V_{o1} of first receiver is highest, as shown in Fig. 15 (b). By changing m_f from 0.5 into 1, as shown in Fig. 14 (c), the frequency component of v_d at f_1 is reduced while other two selected frequency components at f_2 and f_3 are increased. It brings a reduction in V_{o1} and the increase in V_{o2} and V_{o3}. Consequently, the power transfer ratio to receivers is changed.

C. VERIFICATION OF POWER RESDISTRIBUTION

Further experimental results of the power transferred to different receivers along with the system efficiency are shown in Fig. 16, where the value of m_f is changed from 0 to 1.5. As noted in (30), the total output power of three receivers is approximated to the output power at individual resonant frequencies $f_1 = f_c$, $f_2 = f_c + f_m$, and $f_3 = f_c + 2f_m$, which are proportional to $[J_0(m_f)]^2$, $[J_1(m_f)]^2$ and $[J_2(m_f)]^2$, respectively. As the increase of m_f in the range between 0 and 1.5, $J_0(m_f)$ is reduced while $J_1(m_f)$ and $J_2(m_f)$ are increased. Therefore, as shown in Fig. 16, the power P_{o1} transferred to

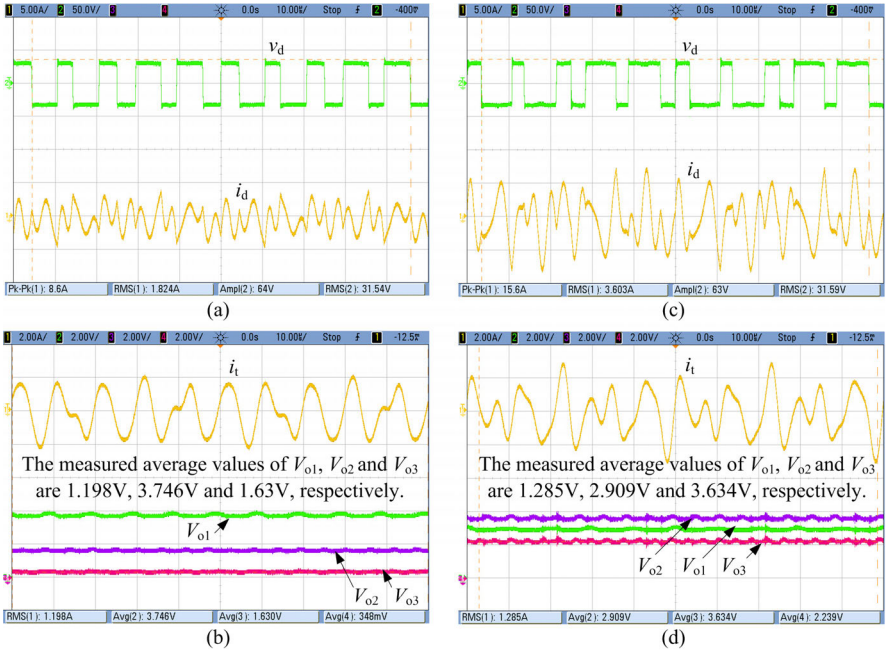

FIGURE 15. Experimental waveforms of the system tested by using CSFM at two different values of m_f ((a) and (b): $m_f = 0.5$; (c) and (d): $m_f = 1$).

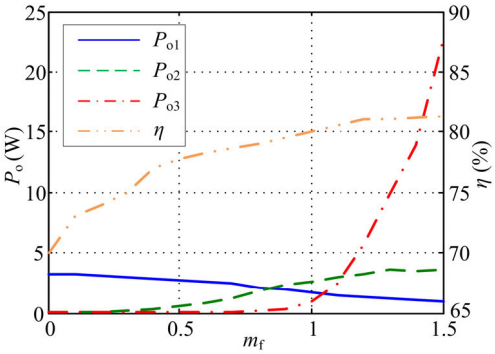

FIGURE 16. Measured power and system efficiency as the change of m_f from 0 to 1.5.

the first receiver becomes smaller and the power P_{o2} and P_{o3} transferred to the second and last receivers become larger. It can be noted in Fig. 16 that P_{o3} increases quickly to a large value after m_f is bigger than 1. As previously addressed, this is because the voltage gain of the designed multi-resonant tank at f_3 is much higher than others at f_1 and f_2. It suggests that m_f should not be chosen too large.

This article focuses on the low power applications, such as mobile phones and swarm robots, where the spatial freedom is tight. Therefore, the size of coils being used in experiments is small and consequently the measured power is not very large. Nevertheless, it does not limit the application of propo- sed system forward to a higher power level. As shown in Fig. 16, just by using the proposed single-inverter-based MF modulation method, any two of receivers can pick up same power and work at the rated power level at the same time. However, since only one modulation degree of freedom is provided in proposed MF modulation method, it would not suitable for more receivers unless the multiple receiving coils are designed with different sizes. The proposed method is particularly suitable to charge the devices of different power levels in a same zone.

VII. CONCLUSION

In this article, a novel and generalized methodology to generate, amplify and compensate the MF power for a single-inverter-based MF-MR-S-WPT system is proposed. The main advantages of proposed methodology include: 1) Based on the proposed CSFM method, a standard full-bridge inverter can be used to generate MF power, leading to a simple configuration of transmitting (Tx) source. 2) With CSFM, a modulation degree of freedom can be provided to change the power transfer ratio, achieving power redistribution among receivers though software implementation. 3) The proposed general design method of multi-resonant transmitting tank is based on circuit synthesis theory and therefore can avoid the use of complicated multiple harmonic analysis. 4) The proposed methodology could be easily extended to the applications with arbitrary multiple receivers. To highlight these advantages, Table 2 shows some comparisons between the proposed and existing MF-MR-S-WPT systems in [11]–[19]. It can be noted that the system that uses the proposed methodology is obviously better than the existing MF-MR-S-WPT systems. Unfortunately, the individual power control cannot be achieved in this article, which will be studied in the future.

APPENDIX A

$$\cos[km_f \sin(\omega_m t)] = J_0(km_f) + 2\sum_{n=2,4,6}^{\infty} J_n(km_f)\cos(n\omega_m t) \quad \text{(A1)}$$

TABLE 2. Comparisons between proposed and existing MF-MR-S-WPT systems.

Ref.	Tx source	Power redistribution implementation	MF power amplification	MF power compensation	Extension to more receivers
[11]	Multiple inverters & multiple transformers	Hardware	No	No	More inverters & transformers
[12]		**Software**	**Yes**	**Yes**	
[13]	Multiple inverters & repeater	Software & Hardware	No	No	More inverters & Tx coils
[14] & [15]	Single inverter & series diode	**Software**	No	No	Limited to three receivers
[16] & [17]	**Single inverter**	No implementation	**Yes**	**Yes**	Limited to two receivers
[18] & [19]	**Single inverter**	**Software**	No	No	Limited to two receivers
Proposed	**Single inverter**	**Software**	**Yes**	**Yes**	**No change in Tx source**

$$\sin[km_{\mathrm{f}}\sin(\omega_{\mathrm{m}}t)] = 2\sum_{n=1,3,5}^{\infty} J_n(km_{\mathrm{f}})\sin(n\omega_{\mathrm{m}}t) \tag{A2}$$

APPENDIX B

According to the Kirchhoff's voltage law, the subsystem composed transmitting coil and multiple receivers can be described as

$$\begin{bmatrix} \dot{V}_{\mathrm{t}} \\ 0 \\ \vdots \\ 0 \end{bmatrix} = \begin{bmatrix} Z_{\mathrm{t}} & \mathrm{j}\omega M_{\mathrm{t}1} & \cdots & \mathrm{j}\omega M_{\mathrm{t}n} \\ \mathrm{j}\omega M_{\mathrm{t}1} & Z_{\mathrm{r}1} & & \mathrm{j}\omega M_{1n} \\ \vdots & & \ddots & \\ \mathrm{j}\omega M_{\mathrm{t}n} & \mathrm{j}\omega M_{1n} & & Z_{\mathrm{r}n} \end{bmatrix} \begin{bmatrix} \dot{I}_{\mathrm{t}} \\ \dot{I}_{\mathrm{r}1} \\ \vdots \\ \dot{I}_{\mathrm{r}n} \end{bmatrix} \tag{A3}$$

where $\dot{V}_{\mathrm{t}}$ and $\dot{I}_{\mathrm{t}}$ are the excitation voltage and current phasors of transmitting coil. $\dot{I}_{\mathrm{r}i}(i = 1, \ldots, n)$ is the current phasor of the ith receiving coil. $Z_{\mathrm{t}} = R_{\mathrm{t}} + \mathrm{j}\,\omega L_{\mathrm{t}}$. $Z_{\mathrm{r}}i = R_{\mathrm{r}}i + R_{\mathrm{rec}i} + \mathrm{j}\omega L_{\mathrm{r}}i + 1/(\mathrm{j}\omega C_{\mathrm{r}}i)$ and $R_{\mathrm{rec}i} = 4R_{\mathrm{L}i}/\pi^2$ is the equivalent input resistance of the ith uncontrollable half-bridge rectifier.

By applying Cramer's rule, the solution of I_{t} can be obtained as

$$I_{\mathrm{t}} = A_1 D / V_{\mathrm{t}} \tag{A4}$$

where D, as given in (A5), is the determinant of $n \times n$ coefficient matrix of (A3) and A_1, as given in (A6), is the determinant of that coefficient matrix with its first row and first column removed.

$$D = \begin{vmatrix} Z_{\mathrm{t}} & \mathrm{j}\omega M_{\mathrm{t}1} & \cdots & \mathrm{j}\omega M_{\mathrm{t}n} \\ \mathrm{j}\omega M_{\mathrm{t}1} & Z_{\mathrm{r}1} & & \mathrm{j}\omega M_{1n} \\ \vdots & & \ddots & \\ \mathrm{j}\omega M_{\mathrm{t}n} & \mathrm{j}\omega M_{1n} & & Z_{\mathrm{r}n} \end{vmatrix} \tag{A5}$$

$$A_1 = \begin{vmatrix} Z_{\mathrm{r}1} & & \mathrm{j}\omega M_{1n} \\ & \ddots & \\ \mathrm{j}\omega M_{1n} & & Z_{\mathrm{r}n} \end{vmatrix} \tag{A6}$$

APPENDIX C

For n-order Cauer network shown in Fig. 5, its T-parameter matrix can be obtained as

$$T = \begin{bmatrix} T_{11} & T_{12} \\ T_{21} & T_{22} \end{bmatrix} = \prod_{i=1}^{n} T_i \tag{A7}$$

where T_i $(i = 1, \ldots, n)$ is the T-parameter matrix of the ith LC circuit in Cauer network and can be calculated by

$$T_i = \begin{bmatrix} 1 - \omega^2 L_{\mathrm{c}i} C_{\mathrm{c}i} & \mathrm{j}\omega L_{\mathrm{c}i} \\ \mathrm{j}\omega C_{\mathrm{c}i} & 1 \end{bmatrix} \tag{A8}$$

REFERENCES

[1] A. K. Swain, S. Devarakonda, and U. K. Madawala, "Modeling, sensitivity analysis, and controller synthesis of multipickup bidirectional inductive power transfer systems," *IEEE Trans. Ind. Informat.*, vol. 10, no. 2, pp. 1372–1380, May 2014.

[2] Y. Bu, T. Mizuno, and H. Fujisawa, "Proposal of a wireless power transfer technique for low-power multireceiver applications," *IEEE Trans. Magn.*, vol. 51, no. 11, pp. 1–4, Nov. 2015.

[3] Y.-J. Kim, D. Ha, W. J. Chappell, and P. P. Irazoqui, "Selective wireless power transfer for smart power distribution in a miniature-sized multiple-receiver system," *IEEE Trans. Ind. Electron.*, vol. 63, no. 3, pp. 1853–1862, Mar. 2016.

[4] M. Fu, T. Zhang, X. Zhu, P. C.-K. Luk, and C. Ma, "Compensation of cross coupling in multiple-receiver wireless power transfer systems," *IEEE Trans. Ind. Informat.*, vol. 12, no. 2, pp. 474–482, Apr. 2016.

[5] U. Pratik, B. J. Varghese, A. Azad, and Z. Pantic, "Optimum design of decoupled concentric coils for operation in double-receiver wireless power transfer systems," *IEEE J. Emerg. Sel. Topics Power Electron.*, vol. 7, no. 3, pp. 1982–1998, Sep. 2019.

[6] K. Lee and D.-H. Cho, "Analysis of wireless power transfer for adjustable power distribution among multiple receivers," *IEEE Antennas Wireless Propag. Lett.*, vol. 14, pp. 950–953, 2015.

[7] L. J. Chen, J. T. Boys, and G. A. Covic, "Power management for multiple-pickup IPT systems in materials handling applications," *IEEE J. Emerg. Sel. Topics Power Electron.*, vol. 3, no. 1, pp. 163–176, Mar. 2015.

[8] M. Liu, M. Fu, Y. Wang, and C. Ma, "Battery cell equalization via megahertz multiple-receiver wireless power transfer," *IEEE Trans. Power Electron.*, vol. 33, no. 5, pp. 4135–4144, May 2018.

[9] H. Yin, M. Fu, M. Liu, J. Song, and C. Ma, "Autonomous power control in a reconfigurable 6.78-MHz multiple-receiver wireless charging system," *IEEE Trans. Ind. Electron.*, vol. 65, no. 8, pp. 6177–6187, Aug. 2018.

[10] M. Fu, H. Yin, M. Liu, Y. Wang, and C. Ma, "A 6.78 MHz multiple-receiver wireless power transfer system with constant output voltage and optimum efficiency," *IEEE Trans. Power Electron.*, vol. 33, no. 6, pp. 5330–5340, Jun. 2018.

[11] F. Liu, Y. Yang, Z. Ding, X. Chen, and R. M. Kennel, "A multifrequency superposition methodology to achieve high efficiency and targeted power distribution for a multiload mcr wpt system," *IEEE Trans. Power Electron.*, vol. 33, no. 10, pp. 9005–9016, Oct. 2018.

[12] Y. Huang, C. Liu, Y. Xiao, and S. Liu, "Separate power allocation and control method based on multiple power channels for wireless power transfer," *IEEE Trans. Power Electron.*, vol. 35, no. 9, pp. 9046–9056, Sep. 2020.

[13] M. Q. Nguyen, Y. Chou, D. Plesa, S. Rao, and J.-C. Chiao, "Multiple-inputs and multiple-outputs wireless power combining and delivering systems," *IEEE Trans. Power Electron.*, vol. 30, no. 11, pp. 6254–6263, Nov. 2015.
[14] W. Liu, K. T. Chau, C. H. T. Lee, C. Jiang, W. Han, and W. H. Lam, "Multi-frequency multi-power one-to-many wireless power transfer system," *IEEE Trans. Magn.*, vol. 55, no. 7, pp. 1–9, Jul. 2019.
[15] W. Liu, K. T. Chau, C. H. T. Lee, C. Jiang, W. Han, and W. H. Lam, "Wireless energy-on-demand using magnetic quasi-resonant coupling," *IEEE Trans. Power Electron.*, vol. 35, no. 9, pp. 9057–9069, Sep. 2020.
[16] Z. Pantic, K. Lee, and S. M. Lukic, "Receivers for multifrequency wireless power transfer: Design for minimum interference," *IEEE J. Emerg. Sel. Topics Power Electron.*, vol. 3, no. 1, pp. 234–241, Mar. 2015.
[17] Z. Pantic, K. Lee, and S. M. Lukic, "Multifrequency inductive power transfer," *IEEE Trans. Power Electron.*, vol. 29, no. 11, pp. 5995–6005, Nov. 2014.
[18] C. Zhao and D. Costinett, "GaN-based dual-mode wireless power transfer using multifrequency programmed pulse width modulation," *IEEE Trans. Ind. Electron.*, vol. 64, no. 11, pp. 9165–9176, Nov. 2017.
[19] D. Ahn and P. P. Mercier, "Wireless power transfer with concurrent 200-kHz and 6.78-MHz operation in a single-transmitter device," *IEEE Trans. Power Electron.*, vol. 31, no. 7, pp. 5018–5029, Jul. 2016.
[20] H. Nguyen and J. I. Agbinya, "Splitting frequency diversity in wireless power transmission," *IEEE Trans. Power Electron.*, vol. 30, no. 11, pp. 6088–6096, Nov. 2015.
[21] R. Narayanamoorthi, A. Vimala Juliet, and B. Chokkalingam, "Cross interference minimization and simultaneous wireless power transfer to multiple frequency loads using frequency bifurcation approach," *IEEE Trans. Power Electron.*, vol. 34, no. 11, pp. 10898–10909, Nov. 2019.
[22] C. Qi, Z. Lang, L. Su, X. Chen, and H. Miao, "Model predictive control for a bidirectional wireless power transfer system with maximum efficiency point tracking," in *Proc. IEEE Int. Symp. Predictive Control Electr. Drives Power Electron. (PRECEDE)*, May 2019, pp. 1–5.
[23] C. Qi, Z. Lang, L. Su, X. Chen, and H. Miao, "Finite-Control-Set model predictive control for a wireless power transfer system," in *Proc. IEEE Int. Symp. Predictive Control Electr. Drives Power Electron. (PRECEDE)*, May 2019, pp. 1–5.
[24] A. C. M. de Queiroz, "A generalized approach to the design of multiple resonance networks," *IEEE Trans. Circuits Syst. I, Reg. Papers*, vol. 53, no. 4, pp. 918–927, Apr. 2006.
[25] R. M. Foster, "A reactance theorem," *Bell Syst. Tech. J.*, vol. 3, no. 2, pp. 259–267, Apr. 1924.
[26] D. Gonzalez, J. Balcells, A. Santolaria, J.-C. Le Bunetel, J. Gago, D. Magnon, and S. Brehaut, "Conducted EMI reduction in power converters by means of periodic switching frequency modulation," *IEEE Trans. Power Electron.*, vol. 22, no. 6, pp. 2271–2281, Nov. 2007.

CHEN QI (Member, IEEE) received the B.S. and Ph.D. degrees in electrical engineering from the School of Electrical Engineering, Dalian University of Technology, Dalian, China, in 2009 and 2014, respectively. From April 2015 to October 2016, he was a Postdoctoral Fellow with the Rolls-Royce@NTU Corporate Laboratory, Nanyang Technological University, Singapore. Since November 2016, he has been an Assistant Professor with the Department of Electrical Engineering, Dalian University of Technology. His research interests include model predictive control and wireless power transfer.

HAN MIAO received the B.Eng. degree in electrical engineering from the Beijing Institute of Technology, Beijing, China, in 2019. He is currently pursuing the M.Sc. degree in electrical engineering with the Dalian University of Technology. His current research interest includes wireless power transfer.

ZHENGYING LANG received the B.Eng. degree in electrical engineering from the Dalian University of Technology, Dalian, China, in 2018, where she is currently pursuing the M.Sc. degree in electrical engineering. Her current research interest includes wireless power transfer.

XIYOU CHEN received the B.Sc., M.Sc., and Ph.D. degrees in electrical engineering from the Harbin Institute of Technology, Harbin, China, in 1982, 1985, and 2000, respectively. From April 2004 to March 2005, he was a Visiting Scholar with the Department of Electrical and Computer Engineering, University of Waterloo, Waterloo, ON, Canada. He is currently a Professor with the School of Electrical Engineering, Dalian University of Technology, Dalian, China. His research interests include matrix converters and wireless power transfer.